Resilient Post-Disaster System Reconfiguration for Multiple Energy Service Restoration

Chengquan Ju
Energy Research Institute @ NTU,
Interdisciplinary Graduate School,
Nanyang Technological University
Singapore, Singapore
Email: juch0002@e.ntu.edu.sg

Shuhan Yao
Institute of Catastrophe Risk Management,
Interdisciplinary Graduate School,
Nanyang Technological University
Singapore, Singapore
Email: syao002@e.ntu.edu.sg

Peng Wang
School of Electrical and
Electronic Engineering,
Nanyang Technological University
Singapore, Singapore
Email: epwang@ntu.edu.sg

***Abstract*—In this paper, a reconfiguration model for load restoration in radial distributed systems which includes multiple energy service is proposed, in which local combined heat and power (CHP) plants can generate electrical and thermal power to meet the demand of critical loads during post-disaster. Maximization of total load restoration has been addressed. After sectionalization by using spanning tree, each microgrid can be fed by one CHP plant to satisfy maximum self-adequacy. Based on the modified IEEE 33-bus radial distribution network, different case studies have been implemented and the proposed model have been validated to be effective. With the proposed model, local CHP generation units can be optimally utilized to restore critical loads with multiple energy requirements, thus catastrophic impacts of the natural hazards on both electrical and thermal energy service can be further minimized.**

***Index Terms*—Resilience, service restoration, system reconfiguration, multiple energy, microgrids.**

NOMENCLATURE

A. Indices and sets

t	Time index.
Δt	Time interval.
i, j	Bus/branch index.
n_g	Number of CHP plants.
$\boldsymbol{T}$	Set of time.
$\widetilde{\boldsymbol{N}}$	Set of buses in the preprocessed network.
$\widetilde{\boldsymbol{L}}$	Set of branches in the preprocessed network.
$\boldsymbol{N_g}$	Set of CHP plants in the network.
$\boldsymbol{N_l}$	Set of loads in the network.
$\boldsymbol{\Lambda}$	Set of electrical load coefficients.
$\boldsymbol{M}$	Set of thermal load coefficients.

B. State Variables

α_{ij}	binary connection indicator from bus i to j.
β_{ij}, β_{ji}	Ancillary binary variables for α_{ij}.
V_i	Voltage magnitude at bus i at t.
P_{ij}^t, Q_{ij}^t	Active and reactive power flowing from bus i to j at t.
$P_{E,i}^t, Q_{E,i}^t$	Electrical active and reactive power of CHP plant at bus i in t.
$P_{L,i}^t, Q_{L,i}^t$	Electrical active and reactive load at bus i in t.
$H_{E,i}^t$	Thermal power of CHP plant at bus i in t.
$H_{L,i}^t$	Thermal load at bus i in t.
H_{ij}^t	Thermal power flowing from bus i to j at t.

C. Parameters

r_{ij}, x_{ij}	Resistance and reactance of branch ij.
η_{ij}	Thermal loss factor of branch ij.
$P_{ij}^{t,max}, P_{ij}^{t,min}$	Electrical branch active power limits from i to j at t.
$Q_{ij}^{t,max}, Q_{ij}^{t,min}$	Electrical branch reactive power limits from i to j at t.
$P_{E,i}^{t,max}$	Maximum of electrical active output of CHP plant at bus i during t.
$Q_{E,i}^{t,max}$	Maximum of electrical reactive output of CHP plant at bus i during t.
V_i^{min}, V_i^{max}	Electrical bus voltage limits at bus i.
$P_{L,i}^{t,max}$	Maximum of electrical active load at bus i during t.
$Q_{L,i}^{t,max}$	Maximum of electrical reactive load at bus i during t.
$H_{ij}^{t,max}, H_{ij}^{t,min}$	Thermal branch power limits from i to j at t.
$H_{E,i}^{t,max}$	Maximum of thermal output of CHP plant at bus i during t.
$H_{L,i}^{t,max}$	Maximum of thermal load at bus i during t.
E_i	Fuel reserve of CHP plant at bus i.
η_i	Electrical/thermal coupling factor of CHP plant at bus i.
λ_i	Weighting coefficient of electrical loads at bus i.
μ_i	Weighting coefficient of thermal loads at bus i.

I. INTRODUCTION

In past few years, power system resilience is gaining ascending attention as a key factor of the infrastructures defense against low-probability incidents what may cause severe impacts, such as natural disasters that would bring significant economical and societal disruptions [1], [2]. The resilience of traditional power systems refers to its ability to withstand extraordinary events robustly, to recover from contingencies rapidly, and to adapt the structure of network and operation status of system to avoid or ease the potential influences of future events with similar impacts. [3], [4].

Recently, research focus has expanded intensively to microgrids, which have the potential capability to provide additional resilience as local resources and black start reserves [2]. Penetration of distributed energy resources and development on decentralized control algorithms have further improved resilience by exploiting their capabilities for fast and efficient restoration [5], [6]. In [7], the resiliency of microgrids is enhanced by re-dispatching the dispatchable generators, batteries and controllable loads. [8] proposes for a multi-microgrid smart distribution system, in which the resilience can be enhanced by a hierarchical management scheme. Similar studies have also been investigated in [9]–[11].

Microgrids integrate distributed generators such as combined heat and power (CHP) generation units to supply the loads of various end-users in a decentralized fashion, in which flexibility can be increased and power grid vulnerability can be reduced [12], [13]. Studies on microgrids involving resiliency have ranged from control logic [14], [15] to system planning [16], [17]. Nevertheless, insufficient consideration has concentrated on two main aspects. Firstly, most of the existing studies have merely considered the electrical network and its resilient-oriented restoration/reconfiguration. System reconfiguration for multiple energy service restoration, such as hybrid electrical and thermal distribution system is still yet to be scrutinized. Secondly, due to increasing complexity of multiple constraints, the existing formulation for multiple energy service restoration in large power systems or even distribution systems, is NP-hard and computationally consuming, which may fail to map a global optimum [18], [19].

In order to address the above problems, the focus of out study is on the strategies to improve post-disaster recovery for multiple energy systems, specifically by using existing distributed generations, typically, CHP plants to restore critical electrical and thermal loads in the distribution network. System reconfiguration for multiple energy service restoration need to be addressed. Multiple energy outages resulted from natural disasters need to be investigated as well, since substantial faults may occur and trigger widespread blackouts and collapses [10].

In this paper, a reconfiguration model for load restoration in radial distribution systems which includes multiple energy service is proposed, in which Local CHP plants can generate electrical and thermal power to meet the demand of distribution system critical loads during post-disaster time frames. After sectionalization by using spanning tree, each microgrid can be fed by one CHP plant to satisfy maximum self-adequacy. The structure of this paper is illustrated as follows. The mathematical model for system reconfiguration including electrical and thermal network is formulated in Section II. In Section III, different scenarios are implemented on a modified IEEE 33-bus radial distribution system and the efficacy of the proposed model is validated through the case studies. Finally, the conclusions are presented in Section VI.

II. Problem Identification for Network Reconfiguration

In this section, the system model formulation for network reconfiguration is illustrated. Reconfiguration of the network topology with CHP plants has the capability to restore the interrupted loads more quickly. During post-disaster time frames, local CHP plants dynamically sectionalize the distribution network into sub-microgrids, where only one CHP plant exists in each microgrid to supply electrical and thermal energy to critical electrical/thermal loads, until the restoration of the main grid is accomplished.

A. Network Reconfiguration

The radial distribution network can be presented with $\boldsymbol{N}$ and $\boldsymbol{L}$ symbolizing the sets of buses and branches, respectively. An undirected graph $\boldsymbol{G} = (\boldsymbol{N}, \boldsymbol{L})$ is employed to present the radial distribution network [20]. $\widetilde{\boldsymbol{G}} = \{\widetilde{\boldsymbol{N}}, \widetilde{\boldsymbol{L}}\}$ is applied to represent the sets of buses and branches for the pre-processed radial distribution network. After network reconfiguration, island buses and branches need to be removed from $\boldsymbol{G}$.

Every bus $i \in \widetilde{\boldsymbol{N}}$ should have only one parent bus. Here the state variable α_l is denoted with two ancillary variables β_{ij} and β_{ji} to represent the connection status for each branch $l \in \widetilde{\boldsymbol{L}}$, which gives constraints in (1)-(6) [21]. Specifically, (1) restricts the distribution network topology to radial structure that no ring connection is allowed. (2) suggests the inclusion of branch l in the spanning tree if $\alpha_l = 1$, whenever either bus j is the parent of bus i ($\beta_{ij} = 1$), or bus i is the parent of bus j ($\beta_{ji} = 1$). (3) de notes the requirement that every bus has just one parent except those who include CHP plants. (4)-(6) denote the binary limits. (7) describes the mapping of α_l from buses to branches. The formulation are as follows:

$$\sum_{l \in \widetilde{\boldsymbol{L}}} \alpha_l = N_n - n_g \tag{1}$$

$$\beta_{ij} + \beta_{ji} = \alpha_l, \forall l \in \widetilde{\boldsymbol{L}} \tag{2}$$

$$\sum_{j \in \phi(i)} \beta_{ij} = 1, \forall i \in \widetilde{\boldsymbol{N}} \backslash \widetilde{\boldsymbol{N}}_{\boldsymbol{g}} \tag{3}$$

$$\beta_{ij} \in \{0, 1\}, \forall i \in \widetilde{\boldsymbol{N}}, j \in \phi(i) \tag{4}$$

$$\alpha_l \in \{0, 1\}, \ l \in \widetilde{\boldsymbol{L}} \tag{5}$$

$$\beta_{ij} = 0, \forall i \in \widetilde{\boldsymbol{N}}_{\boldsymbol{g}}, j \in \phi(i) \tag{6}$$

$$\{\alpha_l : l \in \widetilde{\boldsymbol{L}} \rightarrow \{\alpha_{ij} : i, j \in \widetilde{\boldsymbol{N}}\} \tag{7}$$

where $\phi(i)$ denotes the bus set connected to bus i, and N_n is the total number of buses in $\widetilde{\boldsymbol{N}}$.

B. Electrical Network Constraints

In this paper, the linearized DistFlow model is used to formulate the electrical power flow constraints [22]–[24]. The whole formulation is shown as follows:

$$(r_{ij}P_{ij}^t + x_{ij}Q_{ij}^t)/V_j^t = \alpha_{ij}(V_j^t - V_i^t),\ \forall i,j \in \widetilde{\boldsymbol{N}} \tag{8}$$

$$P_{E,i}^t - P_{L,i}^t = \sum_{j\in\phi(i)} P_{ij},\ \forall i \in \widetilde{\boldsymbol{N}} \tag{9}$$

$$Q_{E,i}^t - Q_{L,i}^t = \sum_{j\in\phi(i)} Q_{ij},\ \forall i \in \widetilde{\boldsymbol{N}} \tag{10}$$

$$P_{ij}^{t,\min}\alpha_{ij} \le P_{ij}^t \le P_{ij}^{t,\max}\alpha_{ij},\ \forall i,j \in \widetilde{\boldsymbol{N}} \tag{11}$$

$$Q_{ij}^{t,\min}\alpha_{ij} \le Q_{ij}^t \le Q_{ij}^{t,\max}\alpha_{ij},\ \forall i,j \in \widetilde{\boldsymbol{N}} \tag{12}$$

$$0 \le P_{E,i}^t \le P_{E,i}^{t,\max},\ \forall i \in \boldsymbol{N_g}, t \in \boldsymbol{T} \tag{13}$$

$$0 \le Q_{E,i}^t \le Q_{E,i}^{t,\max},\ \forall i \in \boldsymbol{N_g}, t \in \boldsymbol{T} \tag{14}$$

$$V_i^{\min} \le V_i^t \le V_i^{\max}, \forall i \in \widetilde{\boldsymbol{N}}, t \in \boldsymbol{T} \tag{15}$$

$$0 \le P_{L,i}^t \le P_L^{t,\max},\ \forall i \in \boldsymbol{N_l}, t \in \boldsymbol{T} \tag{16}$$

$$0 \le Q_{L,i}^t \le Q_L^{t,\max},\ \forall i \in \boldsymbol{N_l}, t \in \boldsymbol{T} \tag{17}$$

$$\sum_{t\in\boldsymbol{T}} P_{E,i}^t \Delta t \le E_i,\ i \in \boldsymbol{N_g} \tag{18}$$

(8) shows the DistFlow equation for connected branches. Specifically, the equality constraint is relaxed by the binary indicator α_{ij} if the branch is disconnected [25]. (9) and (10) describe the node power balance. (11) and (12) denote the branch active and reactive power limits relaxed by α_{ij}, respectively. (13)-(15) refer to the CHP electrical active and reactive outputs and voltage limits, respectively. (16) and (17) restricts the load curtailment ranges due to insufficient power supply in restoration. (18) imposes generation energy constraints such as limited fuel reserves [26], [27].

C. Thermal Network Constraints

The thermal network constraints can be modeled similar to the active power formulation in the electrical network [28], [29]. Additionally, the electrical/thermal coupling effect and the energy fuel limit should be constrained for CHP plants. The formulation is described as follows:

$$H_{E,i}^t - H_{L,i}^t = \sum_{j\in\phi(i)} (H_{ij} + \delta_{ij}|H_{ij}|),\ \forall i \in \widetilde{\boldsymbol{N}} \tag{19}$$

$$0 \le H_{E,i}^t \le H_{E,i}^{t,\max},\ \forall i \in \boldsymbol{N_g}, t \in \boldsymbol{T} \tag{20}$$

$$0 \le H_{L,i}^t \le H_{L,i}^{t,\max},\ \forall i \in \boldsymbol{N_l}, t \in \boldsymbol{T} \tag{21}$$

$$H_{ij}^{t,\min} \le H_{ij}^t \le H_{ij}^{t,\max},\ \forall i,j \in \widetilde{\boldsymbol{N}} \tag{22}$$

$$H_{E,i}^t = \eta_i P_{E,i}^t,\ \forall i \in \boldsymbol{N_g}, t \in \boldsymbol{T} \tag{23}$$

(19) presents the thermal power flow equation for connected branches. The factor coefficient η_{ij} is incorporated to show thermal transmission losses. (20) refers to the CHP thermal outputs. (21) refers to load curtailment ranges. (22) denotes the branch thermal power limits. Finally, (23) determines the coupling effects on electrical and thermal outputs.

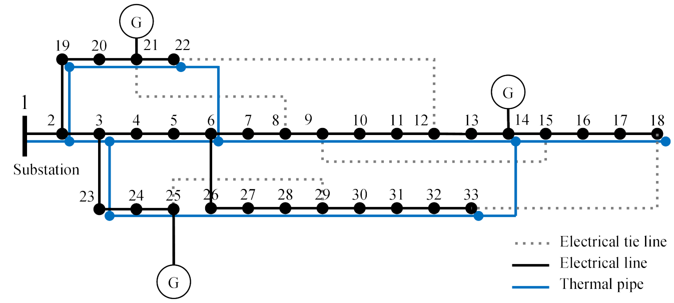

Fig. 1. A modified IEEE 33-bus radial system with local CHP plants.

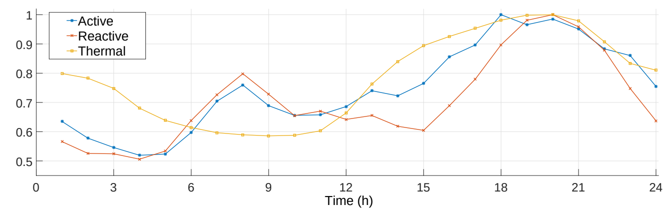

Fig. 2. Normalized load profile in 24h.

D. Objective Function

The objective of the proposed network reconfiguration model is to maximize the service restoration to both electrical and thermal loads on distribution feeders; in other words, to minimize the load loss that is not restored in post-disaster time frames. Two sets of weighting coefficient, $\lambda_i \in \boldsymbol{\Lambda}$ and $\mu_i \in \boldsymbol{M}$, $\forall i \in \boldsymbol{N_l}$, are introduced to show the hierarchical priority of electrical and thermal loads at different nodes, respectively. The objective function can be thus formulated as follows:

$$\begin{aligned} &\min\ -\sum_{t\in T}\sum_{i\in \boldsymbol{N_l}} \left(\lambda_i P_{L,i}^t + \mu_i H_{L,i}^t\right) \\ &\text{subject to}: \\ &\text{Spanning tree constraints}: (2)-(7) \\ &\text{Electrical constraints}: (8)-(18) \\ &\text{Thernal constraints}: (19)-(23) \end{aligned} \tag{24}$$

The above optimization is a non-linear mixed-integer problem, as (8) has non-convex and multiplication terms. Nevertheless, it can be effectively solved by existing solvers such as CPLEX [30] and YALMIP [31] after relaxation to the mixed-integer linear programming. It should be also noted that the reconfigured topological structure is a one-time decision making problem at the initial time of restoration whereas CHP generation can be dispatched at every time step.

III. Case Study and Simulation Results

In this section, a modified IEEE 33-bus radial distribution system is tested to validate the effectiveness of the proposed model. The electrical and thermal system network structure is shown in Fig. 1. It is shown that three local CHP plants are

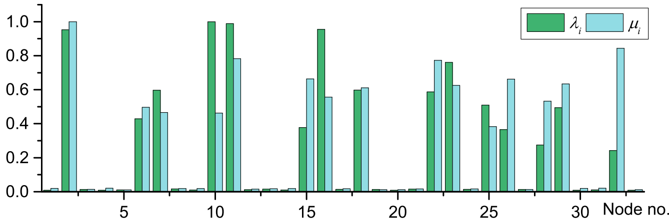

Fig. 3. Electric and thermal load weight coefficients.

TABLE I
CHP PLANT STATISTICS.

Bus no.	P_max(kW)	Q_max(kW)	E_total(kWh)
14	100	50	1200
21	120	60	2020
25	140	70	2350

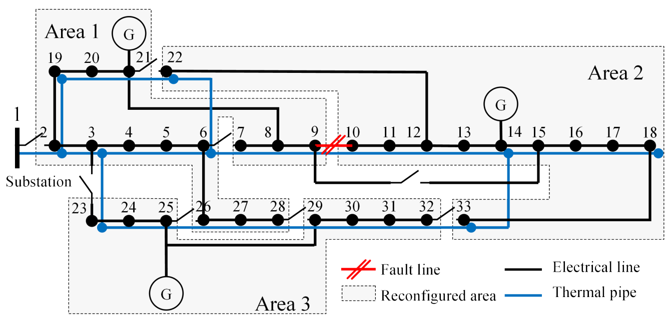

Fig. 4. Reconfigured network structure in Case I.

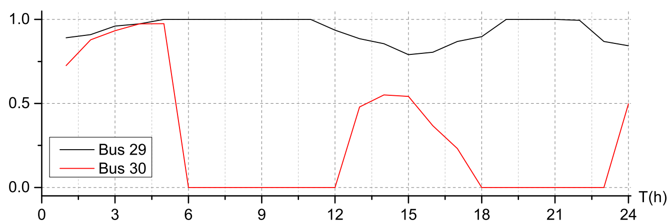

Fig. 5. Normalized electrical load restoration at bus 29 and 30 in Case I.

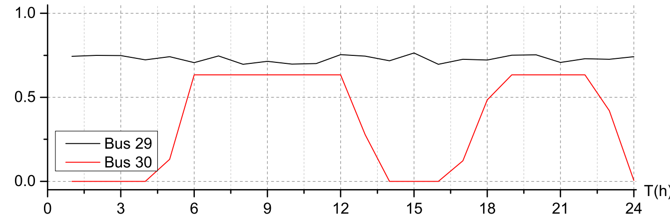

Fig. 6. Normalized thermal load restoration at bus 29 and 30 in Case I.

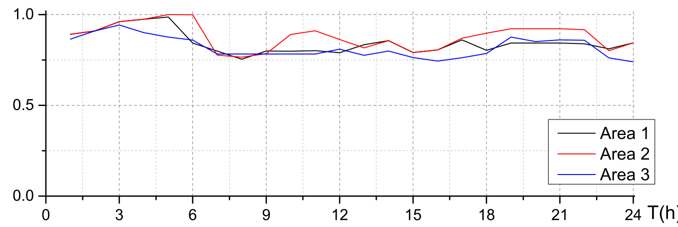

Fig. 7. Normalized electrical load restoration in reconfigured microgrids in Case I.

connected to the original network. The parameters of CHP plants are summarized in TABLE I. As for the electrical and thermal loads, it is assumed that the load is changing over time with corresponding normalized coefficients, as shown in Fig. 2. The weight coefficients for loads at different buses are also presented in Fig. 3. It should be noted that all the configurations are can be adjusted for a variety of scenarios. A 24-hour scheduling horizon simulation is conducted. The optimization model is established using YALMIP [31] with MATPOWER in Matlab [32].

A. Case I: Single Branch Failure

In this case, the branch from bus 9 to bus 10 in the distribution network is disconnected at fault due to natural disastrous events. Fig. 4 shows the reconfiguration network topology for multiple energy restoration with the faulty branch. It is illustrated that the whole distribution system has been isolated automatically from the substation (at bus 1) after the severe contingency. Consequently, the main grid will not be able to power the distribution system, and the remaining area will be supported by local CHP plants during the restoration process, in which there is exactly one CHP plant supplying each sectionalized microgrid by changing the status of branch switches.

Fig. 5 shows the comparison on restored electrical loads at different buses. It is illustrated that due to the relatively priority of bus 30 (as in Fig. 3), some portion of load would be curtailed, while load at bus 29 can be restored at most of time during post-disaster time frames. Differently, thermal load restoration does not strictly follow the predefined priority sequence due to electrical/thermal coupling effects, as shown in Fig. 6. This is also because electrical load and thermal load does not follow the same pattern, as shown in Fig. 3. However, the overall load restoration during the entire horizon at bus 29 is much preferable than that at bus 30.

Furthermore, Fig. 7 shows the normalized electrical load restoration in three reconfigured microgrids, which indicates that load restoration is quite even among different microgrids after system reconfiguration. Note that the thermal network can be considered as the original distribution system, since no disconnection or changing status of tie switches is required.

B. Case II: Multiple Branch Failure

In this case, multiple branch failure in the distribution network is investigated. Several branches (5-6, 8-9, 13-14, 19-20 and 23-24) are disconnected due to failure. Fig. 8 shows the consequential reconfiguration result. It is noticed that there is an isolated zone that does not connect with any microgrid due to multiple faults. Substantially, the normalized electrical

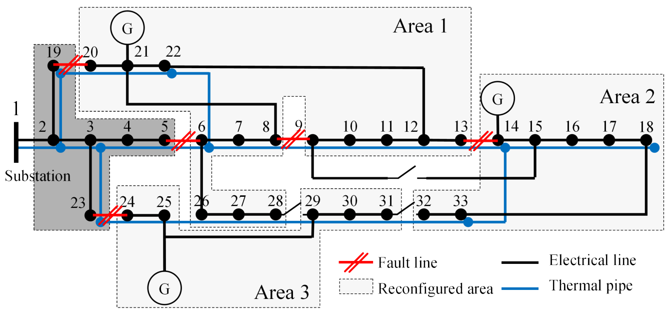

Fig. 8. Reconfigured network structure in Case II.

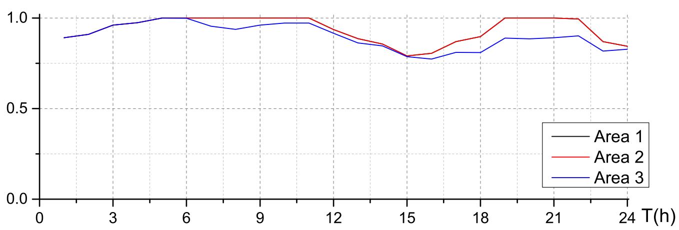

Fig. 9. Normalized electrical load restoration in reconfigured microgrids in Case II.

TABLE II
COMPARISON ON LOAD RESTORATION IN TWO CASES.

Cases	single (case I)	multiple (case II)
Area restoration (electrical)	79.31%	86.62%
Overall restoration (electrical)	78.18%	67.34%
Area restoration (thermal)	76.36%	73.12%
Overall restoration (thermal)	75.02%	72.75%

load restoration in reconfigured microgrids becomes better than that in case I, only because the load in the isolated area has been automatically tripped off. It can be further validated by TABLE. II, which shows the comparison on load restoration in two cases. Specifically, some critical loads with high priority would be curtailed due to limited network power flow constraints. On the other hand, since the topology of the thermal distribution network does not change, the thermal load restoration thus mainly follows the dispatch of electrical resources.

C. Case III: Reconfiguration on Loss of Generator

In case III, the effect of loss of generator is presented, in which the reconfigured network structure after loss of generators are shown in Fig. 10 - Fig. 12. Load restoration levels are also shown in TABLE. III. It can be investigated that the distributed CHP plants can handle most electrical and thermal loads during post-disaster time frames in all three scenarios, except that the curtailed load is mainly limited by the capacity ratings of local CHP plants. Also similar in the above two cases, the influence on the electrical network is much greater than that on the thermal network since the variation of area restoration of electrical load is quite large in

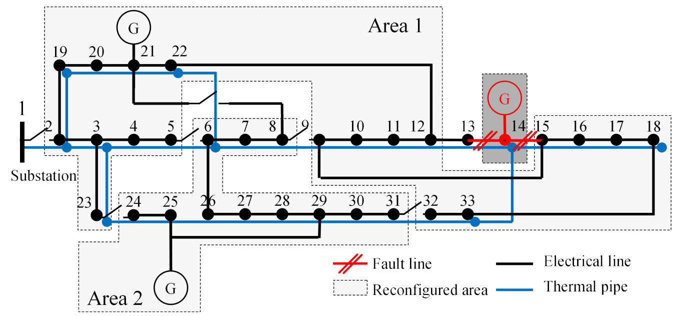

Fig. 10. Reconfigured network structure in Case 3: loss of CHP 1.

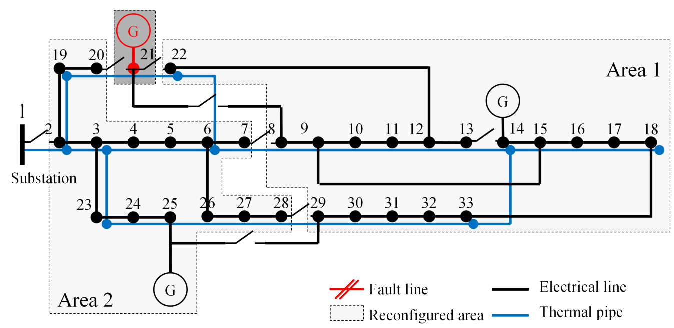

Fig. 11. Reconfigured network structure in Case 3: loss of CHP 2.

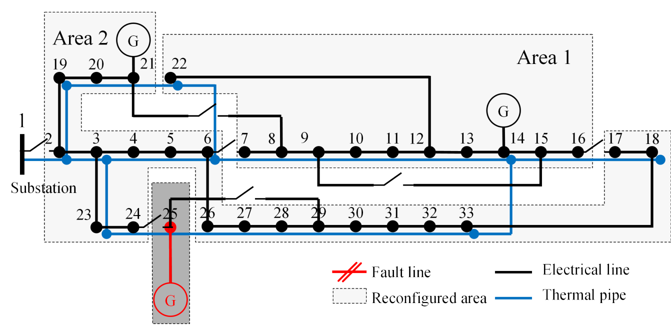

Fig. 12. Reconfigured network structure in Case 3: loss of CHP 3.

TABLE III
COMPARISON ON LOAD RESTORATION IN CASE 3.

Cases	loss of CHP 1	loss of CHP 2	loss of CHP 3
Area restoration (electrical)	68.47%	60.65%	53.36%
Area restoration (thermal)	60.43%	59.45%	53.29%

TABLE. III. This may advice system operators to consider a appropriate design that would deal with worst-case scenarios in the system planning stage.

IV. CONCLUSION

This paper proposes a reconfiguration model for load restoration in radial distribution systems which includes multiple energy service. In post-disaster time frames, local CHP plants can generate electrical and thermal power to meet the demand of critical loads in the system. After sectionalization by using spanning tree, each sectionalized microgrid can be fed by one CHP plant to satisfy maximum self-adequacy. The overall network reconfiguration optimization problem is formulated as a mixed-integer linear programming. Case studies on the modified IEEE 33-bus radial distribution system have validated the effectiveness of the proposed model, that it can optimally utilize local CHP generation units to restore critical loads with multiple energy requirements, thus catastrophic impacts of the natural hazards on both electrical and thermal energy service can be further minimized.

REFERENCES

[1] M. Panteli, D. N. Trakas, P. Mancarella, and N. D. Hatziargyriou, "Boosting the power grid resilience to extreme weather events using defensive islanding," *IEEE Trans. Smart Grid*, vol. 7, no. 6, pp. 2913–2922, 2016.

[2] K. P. Schneider, F. K. Tuffner, M. A. Elizondo, C.-C. Liu, Y. Xu, and D. Ton, "Evaluating the feasibility to use microgrids as a resiliency resource," *IEEE Trans. Smart Grid*, vol. 8, no. 2, pp. 687–696, 2017.

[3] W. House, *Critical Infrastructure Security and Resilience*. White House, 2013.

[4] Y. Xu, C.-C. Liu, Z. Wang, K. Mo, K. P. Schneider, F. K. Tuffner, and D. T. Ton, "Dgs for service restoration to critical loads in a secondary network," *IEEE Trans. Smart Grid*, 2017.

[5] A. Gholami, T. Shekari, F. Aminifar, and M. Shahidehpour, "Microgrid scheduling with uncertainty: the quest for resilience," *IEEE Trans. Smart Grid*, vol. 7, no. 6, pp. 2849–2858, 2016.

[6] H. Liu, R. A. Davidson, and T. V. Apanasovich, "Statistical forecasting of electric power restoration times in hurricanes and ice storms," *IEEE Trans. Power Syst.*, vol. 22, no. 4, pp. 2270–2279, 2007.

[7] A. Hussain, V.-H. Bui, and H.-M. Kim, "Optimal operation of hybrid microgrids for enhancing resiliency considering feasible islanding and survivability," *IET Rene. Power Gen.*, vol. 11, no. 6, pp. 846–857, 2017.

[8] H. Farzin, M. Fotuhi-Firuzabad, and M. Moeini-Aghtaie, "Enhancing power system resilience through hierarchical outage management in multi-microgrids," *IEEE Trans. Smart Grid*, vol. 7, no. 6, pp. 2869–2879, 2016.

[9] A. Khodaei, "Resiliency-oriented microgrid optimal scheduling," *IEEE Trans. Smart Grid*, vol. 5, no. 4, pp. 1584–1591, 2014.

[10] Y. Wang, C. Chen, J. Wang, and R. Baldick, "Research on resilience of power systems under natural disastersa review," *IEEE Trans. Power Syst.*, vol. 31, no. 2, pp. 1604–1613, 2016.

[11] E. Pashajavid, F. Shahnia, and A. Ghosh, "Development of a self-healing strategy to enhance the overloading resilience of islanded microgrids," *IEEE Trans. Smart Grid*, vol. 8, no. 2, pp. 868–880, 2017.

[12] C. Ju, P. Wang, L. Goel, and Y. Xu, "A two-layer energy management system for microgrids with hybrid energy storage considering degradation costs," *IEEE Trans. Smart Grid*, 2017.

[13] K. Rahbar, J. Xu, and R. Zhang, "Real-time energy storage management for renewable integration in microgrid: An off-line optimization approach," *IEEE Trans. Smart Grid*, vol. 6, no. 1, pp. 124–134, 2015.

[19] M. Farivar and S. H. Low, "Branch flow model: Relaxations and convexification," in *2012 IEEE Annu. Conf. on Dec. and Cont.* IEEE, 2012, pp. 3672–3679.

[14] J. Xiao, P. Wang, and L. Setyawan, "Hierarchical control of hybrid energy storage system in dc microgrids," *IEEE Trans. Ind. Electron.*, vol. 62, no. 8, pp. 4915–4924, 2015.

[15] P. Top, M. R. Bell, E. Coyle, and O. Wasynczuk, "Observing the power grid: Working toward a more intelligent, efficient, and reliable smart grid with increasing user visibility," *IEEE Sig. Proc. Mag.*, vol. 29, no. 5, pp. 24–32, 2012.

[16] W. Yuan, J. Wang, F. Qiu, C. Chen, C. Kang, and B. Zeng, "Robust optimization-based resilient distribution network planning against natural disasters," *IEEE Trans. Smart Grid*, vol. 7, no. 6, pp. 2817–2826, 2016.

[17] A. Gholami, F. Aminifar, and M. Shahidehpour, "Front lines against the darkness: Enhancing the resilience of the electricity grid through microgrid facilities," *IEEE Elect. Mag.*, vol. 4, no. 1, pp. 18–24, 2016.

[18] B. D. Ripley, *Stochastic simulation*. John Wiley & Sons, 2009, vol. 316.

[20] Y. Xu, C.-C. Liu, K. Schneider, F. Tuffner, and D. Ton, "Microgrids for service restoration to critical load in a resilient distribution system," *IEEE Trans. Smart Grid*, 2016.

[21] R. A. Jabr, R. Singh, and B. C. Pal, "Minimum loss network reconfiguration using mixed-integer convex programming," *IEEE Trans. Power Syst.*, vol. 27, no. 2, pp. 1106–1115, 2012.

[22] M. E. Baran and F. F. Wu, "Network reconfiguration in distribution systems for loss reduction and load balancing," *IEEE Trans. Power Del.*, vol. 4, no. 2, pp. 1401–1407, 1989.

[23] C. Chen, J. Wang, F. Qiu, and D. Zhao, "Resilient distribution system by microgrids formation after natural disasters," *IEEE Trans. Smart Grid*, vol. 7, no. 2, pp. 958–966, 2016.

[24] T. Ding, Y. Lin, G. Li, and Z. Bie, "A new model for resilient distribution systems by microgrids formation," *IEEE Trans. Power Syst.*, 2017.

[25] J. Li, X.-Y. Ma, C.-C. Liu, and K. P. Schneider, "Distribution system restoration with microgrids using spanning tree search," *IEEE Trans. Power Syst.*, vol. 29, no. 6, pp. 3021–3029, 2014.

[26] H. Gao, Y. Chen, Y. Xu, and C.-C. Liu, "Resilience-oriented critical load restoration using microgrids in distribution systems," *IEEE Trans. Smart Grid*, vol. 7, no. 6, pp. 2837–2848, 2016.

[27] A. Kwasinski, "Quantitative evaluation of dc microgrids availability: Effects of system architecture and converter topology design choices," vol. 26, no. 3, pp. 835–851, 2011.

[28] M. Abeysekera and J. Wu, "Method for simultaneous power flow analysis in coupled multi-vector energy networks," *Ener. Proc.*, vol. 75, pp. 1165–1171, 2015.

[29] J. Söderman and F. Pettersson, "Structural and operational optimisation of distributed energy systems," *Appli. Ther. Engin.*, vol. 26, no. 13, pp. 1400–1408, 2006.

[30] I. I. CPLEX, "V12. 1: Users manual for cplex," *Inter. Bus. Mach. Corp.*, vol. 46, no. 53, p. 157, 2009.

[31] J. Lofberg, "Yalmip: A toolbox for modeling and optimization in matlab," in *2004 IEEE Inter. Sympo. on Comp. Aided Cont. Syst. Design*. IEEE, 2004, pp. 284–289.

[32] R. D. Zimmerman, C. E. Murillo-Sánchez, and R. J. Thomas, "Matpower: Steady-state operations, planning, and analysis tools for power systems research and education," *IEEE Trans. Power Syst.*, vol. 26, no. 1, pp. 12–19, 2011.